



Modelling Magnetar Behaviour with 3D Magnetothermal Simulations

Davide De Grandis^{*,1,2} , Roberto Turolla^{1,2}, Roberto Taverna¹ ,
Toby S. Wood³ and Silvia Zane²

*email: davide.degrandis@phd.unipd.it

¹Department of Physics and Astronomy, University of Padova, via Marzolo 8,
I-35131 Padova, Italy

²Mullard Space Science Laboratory, University College London, Holmbury St. Mary, Surrey,
RH5 6NT, United Kingdom

³School of Mathematics and Statistics, Newcastle University, Newcastle upon Tyne, NE1 7RU,
United Kingdom

Abstract. The observational properties of isolated NSs are shaped by their magnetic field and surface temperature. They evolve in a strongly coupled fashion, and modelling them is key in understanding the emission properties of NSs. Much effort was put in tackling this problem in the past but only recently a suitable 3D numerical framework was developed. We present a set of 3D simulations addressing both the long-term evolution ($\approx 10^4$ – 10^6 yrs) and short-lived outbursts ($\lesssim 1$ yr). Not only a 3D approach allows one to test complex field geometries, but it is absolutely key to model magnetar outbursts, which observations associate to the appearance of small, inherently asymmetric hot regions. Even though the mechanism that triggers these phenomena is not completely understood, following the evolution of a localised heat injection in the crust serves as a model to study the unfolding of the event.

Keywords. neutron stars, magnetic fields, numerical methods

1. Introduction

We present a set of simulations of the magnetic and thermal evolution in a NS crust performed with a suitably adapted version of the 3D code *PARODY* (Wood & Hollerbach 2014). We restrict the integration domain to the NS crust only, relying on the assumption of complete magnetic flux expulsion from the superconducting core. The core of the star is treated as a boundary condition in prescribing the temperature at the crust bottom. The evolution of the crust is computed by solving the Hall induction equation in the electron MHD regime (i.e. one in which only electrons can move), and the heat balance equation

$$\frac{\partial \mathbf{B}}{\partial t} = -c \nabla \times \left[\sigma^{-1} \mathbf{J} + \frac{1}{ecn_e} \mathbf{J} \times \mathbf{B} + \mathbf{G} \cdot \nabla T - \frac{\nabla \mu}{e} \right] \quad (1.1)$$

$$C_v \frac{\partial T}{\partial t} = -\nabla \cdot \left(T \mathbf{G} \cdot \mathbf{J} - \mathbf{k} \cdot \nabla T - \frac{\mu}{e} \mathbf{J} \right) + \mathbf{E} \cdot \mathbf{J} - N_\nu \quad (1.2)$$

where \mathbf{B} and \mathbf{E} are the magnetic and electric field, T is the temperature, n_e is the electron density, $\mu = c\hbar(3\pi^2 n_e)^{1/3}$ is the electron chemical potential, $\mathbf{J} = c\nabla \times \mathbf{B}/4\pi$ is the current, \mathbf{k} is the thermal conductivity tensor, \mathbf{G} is the thermopower tensor and C_v is the heat capacity (per unit volume). The electrical and thermal conductivity σ and \mathbf{k} are

taken as those of a completely degenerate gas of electrons (see [De Grandis et al. \(2020\)](#) for a complete description of the code and microphysical input). N_ν is the neutrino emissivity due to weak processes in the crust ([Yakovlev et al. 2001](#); we considered the contributions from weak plasmon decay, neutrino bremsstrahlung, weak pair annihilation and weak synchrotron emission). Contrary to neutrino emission from the core, that regulates the thermal evolution throughout the NS life, crustal processes become active above $\sim 3 \times 10^9$ K; therefore, they are important only in the early cooling phases or during transient activity due to large heat deposition in the crust. We computed the luminosity of the star (in the local rest frame) assuming patch-wise blackbody emission at the local surface temperature. Note that the latter is different from the temperature at the top of the crust due to the presence of a (magnetised) blanketing envelope (e.g. [Bezgonov et al. 2021](#)), which also sets the boundary condition for Eq. 1.2.

We studied the long-term evolution adopting the equation of state from [Gourgouliatos & Cumming 2014](#) that describes the inner crust only, i.e. assuming a thick blanketing envelope; to describe short term phenomena we added the outer layers of the crust up to $\approx 10^7$ g cm $^{-3}$, using the profile proposed by [Yakovlev et al. \(2021\)](#) (see their Eq. 2) for standard NS parameters, $M = 1.4 M_\odot$, $R = 12$ km.

2. Secular Evolution Models

We first consider the evolution of a purely dipolar initial field (Fig. 1) with $B_d \simeq 10^{13}$ G. In the first $\approx 10^5$ yr, the evolution is dominated by the Hall term, which displaces energy to the smaller scales. In particular, it tends to favour odd multipoles, pointing to a structure known as the *Hall attractor* ([Gourgouliatos & Cumming 2014](#)). We found that this configuration produces stronger field structures around the magnetic equator, where closed lines get formed. In turn, this translates into the appearance of a hot equatorial belt: in fact, not only the field ohmic decay heats the crust, but due to the anisotropic conductivity, which is favoured along the field lines, the magnetic loops act as a thermal insulator. Note, however, that the presence of a magnetised envelope makes so that the crustal thermal structure does not directly map to the surface: in fact, at the equator the field is parallel to the surface, thwarting heat transport in the blanketing envelope. The result is a cold equatorial belt, whereas the polar regions are initially warmer. After the equatorial heat trapping has been active for a long time, however, hot structures appear around the cold equatorial belt, with intermediate temperature polar caps. If the field is not symmetric, this mechanism is not as efficient. We ran a simulation with a field composed initially of a dipolar field and a quadrupolar one tilted by an angle $\Theta_q = 45^\circ$. In this case, a hot structure appears around the equator of the dipole, but it is asymmetric, having an almost spot-like appearance. The effect of the envelope still produces a cold belt, which is skewed by the asymmetric field. The thermal map can then be used to simulate the emission observables using a GR ray-tracing code ([Taverna et al. 2015](#)). The pulsed fraction can reach $\lesssim 20\%$, whereas in the dipolar case it is $\lesssim 5\%$.

3. Short-term evolution & Magnetar Outbursts

Magnetars are the most strongly magnetised NSs and are characterised by violent activity in the X/ γ -rays. In particular, many of them exhibit *outbursts*, sudden (\approx hours) increases of the flux (by a factor 10-1000 with respect to the quiescent level), accompanied by a modification of the X-ray spectrum and of the pulse profile. These are interpreted as the appearance of hotter region(s) on the star surface, that then decay over several months (see [Coti Zelati et al. \(2018\)](#) for a comprehensive overview of outburst properties). In order to model this behaviour, we used the version of the code adapted to short-term events, injecting heat in a localised patch in the outer crust ($\rho \simeq 3 \times 10^7$ g cm $^{-3}$). The

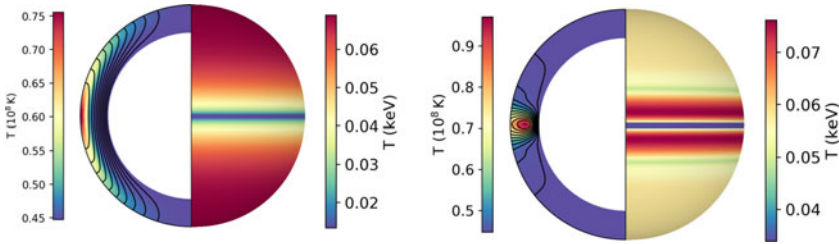
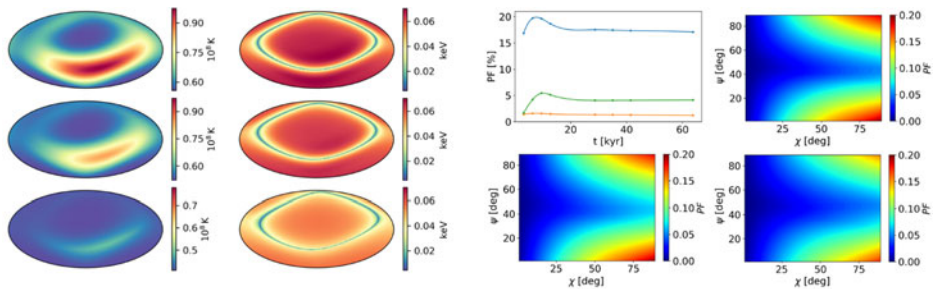


Figure 1. Two snapshots at $t \approx 2$ kyr and $t \approx 400$ kyr of the evolution of the temperature and poloidal field in an initially dipolar case. The left half of each plot shows the temperature structure inside the crust (enlarged for visualisation), with the field lines superimposed; the right half the corresponding surface thermal map, considering the blanketing envelope (from De Grandis *et al.* 2021).



(a) Mollweide projection of the thermal maps at the top of the crust (left) and at the surface (right).

(b) Evolution of the PF for selected viewing angles, alongside its full dependence on ξ and ψ at selected times.

Figure 2. Thermal maps and pulsed fractions a field with $B_{\text{quad}}/B_{\text{dip}} = 1.25$, $\Theta_q = 45^\circ$, shown at three times (increasing from top to bottom, left to right). The PF evolution is shown for different viewing geometries (from De Grandis *et al.* 2021).

injection was performed over a short time (\approx minutes); we verified that the exact duration of the injection is irrelevant, as long as it is shorter than ≈ 1 hour and the total injected energy is the same. We studied the effect of neutrino emission by increasing the amount of heat in the same patch, comprising $\sim 3\%$ of the total volume and $\sim 20\%$ of the surface. As crustal neutrino emission gets triggered above $\simeq 3 \times 10^9$ K, more and more heat gets dissipated via this channel rather than carried away by surface photon emission. Hence, the peak luminosity saturates, as shown in Fig. 3. Moreover, the effect of the magnetic field is particularly evident considering different geometries of the field itself. The same patch of $\simeq 5$ km radius heated with $H \simeq 4 \times 10^{40}$ erg, yields very different lightcurves when located at the magnetic pole or across the equator, again due to the thermally insulating effect of the field. The shape of the emerging hotspot is also different in the two cases, see Fig. 4. In the models considered above, we took a field $B \simeq 10^{13}$ G as a representative value. This choice is not restrictive, since we found that models with fields in a range $\approx 10^{12}$ G– 10^{14} G yield lightcurves that only differ quantitatively between each other. In particular, their timing properties (rise-onset and peak times) showed no variations in all the cases we considered.

Our work has shown the key role of the magnetic field in shaping the observed properties of NSs both in the long and the short term and highlighted the importance of 3D simulations in providing a thorough assessment of the different aspects of NS magnetothermal evolution.

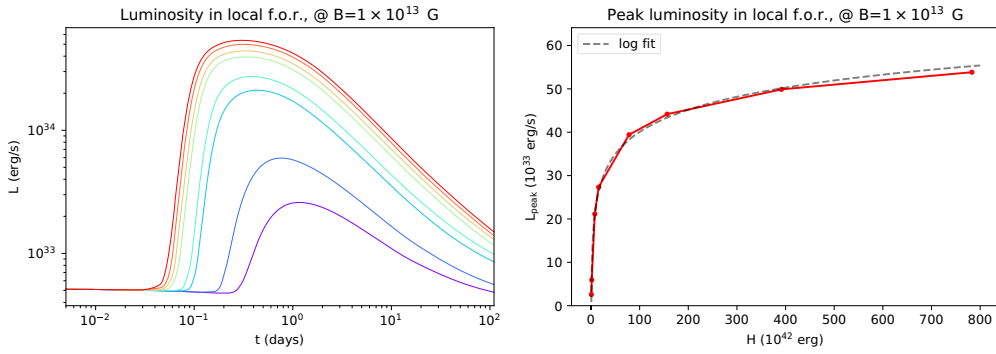


Figure 3. (Left panel) Luminosity curves after the injection of increasing amounts of heat; higher curves correspond to higher H for a NS with $T(0) = 10^8$ K, $B \simeq 10^{13}$ G. (Right panel) Peak luminosity as a function of the heat injection. A logarithmic fit to the points has been added as a reference.

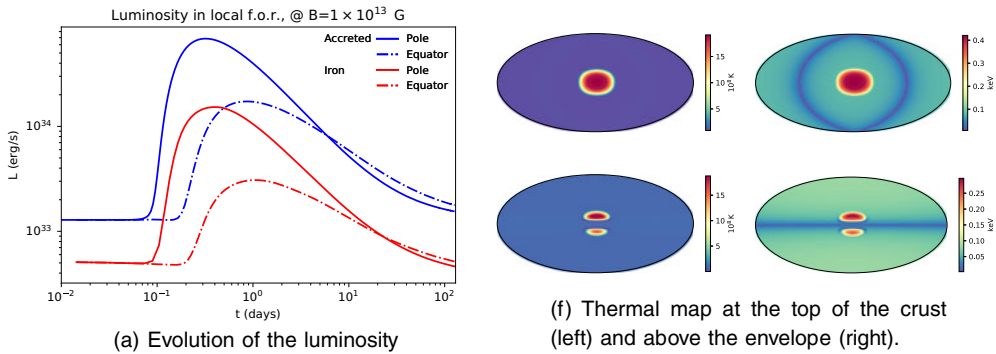


Figure 4. Outburst models for a NS with $B = 10^{13}$ G and an injection of $H \simeq 4 \times 10^{40}$ erg in two different positions w.r.t. the dipolar field, around the pole (continuous lines) and across the equator (dot-dashed lines). Two different envelope compositions are considered, Fe-Ni (red curves) and a light-element (blue curves, [Bezgonov et al. 2021](#)). The thermal maps are shown after $t = 9$ h (rise phase) for the Fe-Ni envelope. The top row shows the case of polar injection (pole towards the observer), the bottom one equatorial injection (pole upwards).

References

- Beznogov M. V., Potekhin A. Y., Yakovlev, D. G. 2001, *Phys. Rep.*, 919:168. doi: 10.1016/j.physrep.2021.03.004.
- Coti Zelati, F., Rea N., Pons, J. A., Campana S., Esposito, P. 2018, *MNRAS*, 474(1):961–1017. doi: 10.1093/mnras/stx2679.
- De Grandis, D., Turolla, R., Wood, T. S., Zane, S., Taverna, R., Gourgouliatos, K. N. 2020, *ApJ* 903(1):40. doi: 10.3847/1538-4357/abb6f9.
- De Grandis, D., Taverna, R., Turolla, R., Gnarini, A., Popov, S. B., Zane, S., Wood, T. S. 2021, *ApJ* 914(2):118. doi: 10.3847/1538-4357/abfdac.
- Gourgouliatos, K. N., Cumming, A. 2014, *Phys. Rev. Lett.*, 112(17):171101. doi: 10.1103/PhysRevLett.112.171101.
- Taverna, R., Turolla, R., Gonzalez Caniulef, D., Zane, S., Muleri, F., Soffitta, P. 2015, *MNRAS*, 454(3):32543266. doi: 10.1093/mnras/stv2168.
- Wood, T. S., Hollerbach, R. 2015, *Phys. Rev. Lett.*, 114(19):191101. doi: 10.1103/PhysRevLett.114.191101.
- Yakovlev, D. G., Kaminker, A. D., Gnedin, O. Y., Haensel, P. 2001, *Phys. Rep.* 354(1-2):1–155. doi: 10.1016/S0370-1573(00)00131-9.
- Yakovlev, D. G., Kaminker, A. D., Potekhin, A. Y., Haensel, P. 2021 *MNRAS* 500(4):4491–4505. doi: 10.1093/mnras/staa3547.